

LETTER TO THE EDITOR

# Spatially resolved 4.7 $\mu\text{m}$ CO fundamental emission in two protoplanetary disks<sup>★</sup>

G. van der Plas<sup>1,2</sup>, M. E. van den Ancker<sup>1</sup>, B. Acke<sup>3,★★</sup>, A. Carmona<sup>4</sup>, C. Dominik<sup>2,5</sup>, D. Fedele<sup>6</sup>, and L.B.F.M. Waters<sup>2,3</sup>

<sup>1</sup> European Southern Observatory, Karl-Schwarzschild-Str.2, D 85748 Garching bei München, Germany

<sup>2</sup> Sterrenkundig Instituut 'Anton Pannekoek', University of Amsterdam, Kruislaan 403, 1098 SJ Amsterdam, The Netherlands

<sup>3</sup> Department of Physics and Astronomy, KU Leuven, Celestijnenlaan 200D, 3001 Leuven, Belgium

<sup>4</sup> ISDC Data Centre for Astrophysics, Ch. d'Ecogia 16, 1290 Versoix, Switzerland

<sup>5</sup> Institute for Astrophysics, Radboud University, Heyendaalseweg 135, 6525 AJ Nijmegen, The Netherlands

<sup>6</sup> Max-Planck-Institut für Astronomie, Königstuhl 17, 69117 Heidelberg, Germany

## ABSTRACT

**Aims.** We investigate the physical properties of the gas in the disks around the Herbig Ae/Be stars HD 97048 and HD 100546.

**Methods.** Using high-spectral-resolution 4.6-5.1  $\mu\text{m}$  spectra containing fundamental CO emission taken with the CRIRES on the VLT, we probe the physical properties of the circumstellar gas and model the kinematics of the emission lines. By using spectro-astrometry on the spatially resolved targets, we constrain the physical size of the emitting regions in the disks.

**Results.** We resolve, spectrally and spatially, the emission of the <sup>13</sup>CO v(1-0) vibrational band and the <sup>12</sup>CO v(1-0), v(2-1), v(3-2) and v(4-3) vibrational bands in both targets, as well as the <sup>12</sup>CO v(5-4) band in HD 100546. The spectro-astrometry yields shifts in the photo center for all spatially resolved vibrational lines in HD 100546 up to between 9 and 10 AU, and for HD 97048 up to 16 AU for the v(2-1) and v(3-2) vibrational lines. Modeling of the CO emission yields inner radii of the CO emitting region of 12 and 15 AU for HD 97048 and HD 100546 respectively. The fact that continuum emission is present within these radii in both stars and gaseous [OI] emission was previously detected in both targets at smaller radii suggests that CO may be effectively destroyed at small radii in the surface layers of the disks surrounding intermediate-mass young stars. The CO emitting regions of both stars are comparable, but the continuum emission of HD 100546 originates from an area half the size of the HD 97048 continuum emission.

**Key words.** circumstellar matter, stars – pre-main-sequence, stars – HD 97048, stars – HD 100546, protoplanetary disks

## 1. Introduction

We present a study of warm carbon monoxide (CO) gas in two circumstellar disks surrounding young intermediate-mass stars. CO is the second most abundant molecule in the universe after H<sub>2</sub> and commonly detected in disks (Najita et al., 2003). In contrast to H<sub>2</sub>, the rotational transitions of CO are much stronger, and hence easier to detect. Therefore CO is often used as a tracer of gas in disks. Ro-vibrational transitions of warm (T = 120-1010 K) CO gas have already been found by Mitchell et al. (1990) in 8 out of 9 surveyed embedded infrared sources. Brittain et al. (2007) had a 100 % detection rate for the ro-vibrational CO transitions in the disks around 9 intermediate mass stars with optically thick inner disks, while their detection rate is only 1 out of 5 for disks with an optically thin inner disk, a case they explain by UV fluorescence. Recently, Pontoppidan et al. (2008) have spatially and spectrally resolved the 4.7  $\mu\text{m}$  CO ro vibrational lines in the disks around 3 young solar mass stars with known dust gaps or inner holes, and detected CO well inside the dust gaps in all disks.

HD 97048 (Sp. type A0pshe) is a well-studied nearby Herbig star, whose spectral energy distribution (SED) displays a large infrared excess above the emission from the star, commonly ex-

plained by emission from warm dust in a circumstellar disk. The disk is a flaring disk according to the classification proposed by Meeus et al. (2001). Lagage et al. (2006) resolved the disk around HD 97048 in the mid-IR and determined the flaring angle. PAH emission from radii up to 200-300 AU has been detected by van Boekel et al. (2004). Habart et al. (2004) have resolved emission from the 3.43  $\mu\text{m}$  and 3.54  $\mu\text{m}$  nanodiamond bands from within the inner 15 AU in the disk. Circumstellar gas has also been detected, e.g. by Acke & van den Ancker (2006) who detect [OI] emission at radii between 0.5 and 60 AU from the central star. HD 97048 is one of the only two Herbig stars where the H<sub>2</sub> S(1) line at 17.035  $\mu\text{m}$  has been detected (Martin-Zaïdi et al., 2007), coming from warm gas within 35 AU.

HD 100546 (Sp. type B9Vne) has a SED typical for a flaring disk, and its disk processes a high crystalline silicate dust fraction (Bouwman et al., 2003). The circumstellar disk has a gap, or 'secondary wall',  $\approx$  10 AU from the central star, detected from e.g. modeling the SED (Bouwman et al., 2003), and [OI] emission, possibly induced by a very low mass stellar companion or planet of  $\approx$  20  $M_{\text{Jup}}$  (Acke & van den Ancker, 2006). The latter authors also resolved the [OI] emission to originate from between 0.5 and 60 AU. Geers et al. (2007) have detected PAH emission from  $12 \pm 3$  AU, and the circumstellar material has been resolved many times, revealing rich structures in the disk.

Send offprint requests to: G. van der Plas, e-mail: gvanderp@eso.org

<sup>★</sup> Based on observations collected at the European Southern Observatory, Paranal, Chile. (Program ID 079.C-0349A)

<sup>★★</sup> Postdoctoral Fellow of the Fund for Scientific Research, Flanders.

**Table 1.** Astrophysical parameters of the programme stars

HD	$\log T_{\text{eff}}$ $\log [\text{K}]$	$\log L_{\text{bol}}$ $\log [L_{\odot}]$	M $[M_{\odot}]$	Dist. $[\text{pc}]$	i $[^{\circ}]$	PA $[^{\circ}]$
97048	4.00	1.42	$2.5^{+0.2}$	$180^a$	$42.8^{+0.8,b}$	$160^{\pm 19,c}$
100546	4.02	1.62	$2.4^{\pm 0.1}$	$103^a$	$42^{\pm 5,d}$	$145^{\pm 5,d}$

<sup>a</sup> van den Ancker et al. (1998)    <sup>b</sup>Lagage et al. (2006)  
<sup>c</sup>Acke & van den Ancker (2006)    <sup>d</sup>Ardila et al. (2007)

In this letter, we present milli-arc-second precision observations of the 4.6-5.1  $\mu\text{m}$  fundamental CO emission originating from the disks around HD 97048 and HD 100546.

## 2. Observations and data reduction

High-spectral-resolution ( $R \approx 94000$ ) spectra of HD 97048 and HD 100546 were obtained on the early morning of June 16<sup>th</sup> 2007 with the VLT cryogenic high-resolution infrared echelle spectrograph (CRIRES<sup>1</sup>, Käuffel et al. (2004)). Adaptive Optics were used to optimize the signal-to-noise and the spatial resolution of the observations. They cover the wavelength range of 4.588 - 4.810  $\mu\text{m}$  and 4.950 - 5.095  $\mu\text{m}$ , and contain many of the fundamental ro-vibrational transitions of the CO molecule. The observations were made with a slit width of 0.2", and with the slit rotated along the parallactic angle. HD 97048 and HD 100546 were observed with 6 wavelength settings, each for resp. 10 and 3 minutes, and the observations span a range in Position Angle (PA) of 41.1 - 64.7 degrees for HD 97048 and 74.8 - 80.5 degrees for HD 100546. The data were reduced using the CRIRES pipeline V1.5.0<sup>2</sup>, which performs wavelength calibration, background subtraction and flatfield correction.

To correct for telluric absorption we have observed a telluric standard directly after each science target. These standards were chosen to be as close as possible on the sky so that their spectra are affected by similar atmospheric conditions, and are HIP 052419 (Sp. type B0V) for HD 97048 and HIP 061585 (Sp. type B2IV) for HD 100546. We compared their spectra with a Kurucz (1991) stellar atmosphere model appropriate for each star to correct for the instrumental response. After scaling the science- and standard-star so that their telluric absorption lines have comparable optical depth, we manually align both spectra in wavelength on their telluric absorption lines and divide them. Some telluric absorption lines are fully saturated, causing problems with the division of the spectra (i.e. division by 0). In the further data reduction, we will disregard these areas. Finally, we corrected the spectra for their radial and barycentric velocity and manually center the <sup>12</sup>CO  $\nu(2-1)$  lines on their rest wavelength to suppress the residuals in the wavelength calibration. The spectra are shown in Fig. 1.

## 3. Analysis

To check whether the targets are spatially resolved, we use spectro-astrometry on the raw 2D frames. We determine the location of the photo center of the PSF and the spatial FWHM as function of wavelength (or equivalently velocity for each line), by fitting a Gaussian to the spatial profile in each spectral column. The relative shift in Spatial Peak Position (= photo center) with respect to the continuum will be referred to in this paper

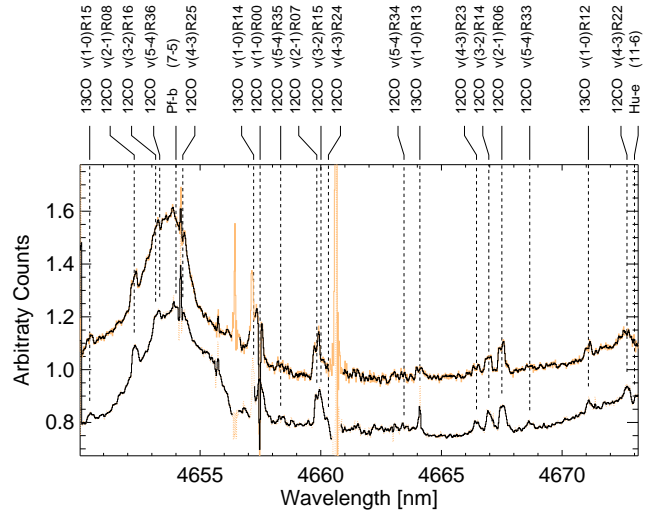


**Fig. 1.** Reduced CRIRES spectra of HD 97048 (top) and HD 100546 (bottom). The black spectrum has been used for the line measurements, whereas the red line shows the areas that have been ignored due to high errors, mostly caused by the correction for saturated telluric lines. The line identifications plotted above show detections of the isotope (<sup>13</sup>CO and <sup>12</sup>CO), the vibrational transition (e.g.  $\nu(1-0)$ ), and the rotational transition ( $R_{xx}$  or  $P_{xx}$ ). The broad hydrogen recombination lines Pfund  $\beta$  at 4654 nm and Humphrey  $\epsilon$  at 4673 nm are also shown.

as the SPP, and is a measure for the spatial offset of the emitting region compared to the continuum. Our observations are made with the slit positioned at only one position angle (PA). We note that Pontoppidan et al. (2008) have observed three nearby T Tauri stars at 6 different PA's with CRIRES and the same observational set-up as employed by us, and find the reverse astrometric signal between slit orientations rotated by 180°. We thus assume the spectro-astrometric signal in our data to be real and not to be due to instrumental artifacts. We compare the SPP in the CO lines to the SPP of the underlying continuum (SPP=0 by definition). If the target is resolved, and the photo center of the CO emission region is significantly offset to that of the dust disk, the SPP is expected to be non-zero. The real photo center displacement can be derived from the measured SPP if we correct for dilution by the continuum emission. Following Pontoppidan et al. (2008), we correct by multiplying the SPP with a factor  $1 + F_c(\nu)/F_l(\nu)$ , with  $F_c(\nu)$  and  $F_l(\nu)$  the continuum and line flux at velocity  $\nu$ .

The Gaussian fit to the PSF also yields a spatial FWHM. If the continuum is unresolved (in case of the telluric standards), this quantity is a measure for the achieved effective spatial resolution in the direction parallel to the slit. When resolved (in case of the science targets), the FWHM allows us to determine the spatial extent of the emission. Outside the spectral lines it then is a direct probe for the size of the continuum emitting disk, whilst inside the lines it is a function of both the line- and continuum emission, and its value is an under limit of the CO emission. Thus measuring the SPP and the FWHM of the PSF in the continuum and the CO lines, allows us to determine the size of the continuum emitting region on the sky, and the spatial offset of each CO line with regard to the continuum. This procedure is shown in Figs. 2 and 3. The data displayed in the figures has been taken with a  $\lambda_c$  of 4676.1 nm. The wavelength setting of

<sup>1</sup> <http://www.eso.org/sci/facilities/paranal/instruments/crises/>

<sup>2</sup> <http://www.eso.org/sci/data-processing/software/pipelines/index.html>

**Table 2.** Spatial information for the *averaged* vibrational transitions shown in Figs 4 and 5, and the radii used to model the kinematics.

HD 97048	cont.	v(2-1)	v(3-2)	v(4-3)	$R_{\text{in/out}}^{\text{model}}$
SPP [AU]	0	$18.2^{\pm 0.9}$	$22.1^{\pm 2.7}$	-	12
FWHM [AU] <sup>a</sup>	$21.2^{\pm 1.6}$	$\geq 23.8^{\pm 1.1}$	$\geq 23.0^{\pm 1.1}$	-	45
HD 100546					
SPP [AU]	0	$10.0^{\pm 0.5}$	$8.7^{\pm 0.5}$	$9^{\pm 1.5}$	15
FWHM [AU]	$10.0^{\pm 0.9}$	$\geq 13.7^{\pm 0.6}$	$\geq 13.1^{\pm 0.6}$	$\geq 11.5^{\pm 0.7}$	40

<sup>a</sup> Note that this FWHM is a function of continuum + line emission, but that the SPP has been corrected for the continuum dilution, and thus is a function of the line emission.

4661.1 nm shows, within observational errors, exactly the same astrometric signal for all CO lines.

An independent method to determine the extent of the emitting gas is to use the kinematics of the line profiles. We construct the average line profile for the v=(1-0) to v(4-3) bands with comparable strengths, and fit these with model a to determine the inner and outer radius of the emission. In our model, we assume that the gas orbits in keplerian rotation, in a disk with known inclination and PA around a star with known stellar mass and distance. Further, the intensity of the emission decreases as  $I(R) = I_{\text{in}} \left(\frac{R}{R_{\text{in}}}\right)^{-\alpha}$ , with  $I_{\text{in}}$  the intensity at the inner radius  $R_{\text{in}}$ ,  $R$  the radial distance from the star, and  $\alpha = 2.5$ . A complete description of the model can be found in Carmona et al. (2007). The free parameters are the inner and outer radius of the emitting gas and can be found in Table 2. The value of the outer radius has a subtle effect on both the line profile and astrometric signal, and should be interpreted as a lower limit to the outer radius. With the parameters thus derived we simulate the expected astrometric signal.

## 4. Results

We detect in the spectrum of **HD 97048** the  $^{13}\text{CO}$  v(1-0), as well as in the  $^{12}\text{CO}$  v(1-0) to v(4-3) vibrational bands. All lines are spectrally resolved. Average line profiles of the  $^{12}\text{CO}$  v(1-0) to v(3-2), and astrometric signals of the latter two transitions are given in Fig. 4 and Table 2. We note that the FWHM denotes the combination of the FWHM of the continuum + line, and is a lower limit for the spatial extent of the line emission. The 4.6  $\mu\text{m}$  continuum emission of the disk around HD 97048 is resolved, and has a FWHM of  $0.231'' \pm 0.004''$ , compared to a FWHM of  $0.198'' \pm 0.003''$  for the unresolved telluric standard. The red- and blue- shifted wings form a sinusoidal signal, typical for an inclined circumstellar disk.

In the spectrum of **HD 100546** we detect the  $^{13}\text{CO}$  v(1-0), as well as in the  $^{12}\text{CO}$  v(1-0) to v(5-4) vibrational bands. All lines are spectrally resolved. The average line profiles and astrometric signals of the  $^{12}\text{CO}$  v(1-0) to v(4-3) transitions are shown in Fig. 5 and Table 2. The 4.6  $\mu\text{m}$  continuum emission of HD 100546 is resolved and has a FWHM of  $0.218'' \pm 0.002''$ , compared to a FWHM of  $0.195'' \pm 0.003''$  for the telluric standard. The SPP is very asymmetric, i.e the negative shift of the blue wing in the SPP is larger than the positive SPP of the red wing. This asymmetry is also seen in the FWHM.

We have, for each vibrational transition, constructed both the average line- and astrometric signal of lines with comparable strengths, and fit both to the model described in section 3, to constrain the location of the emitting gas. We use the param-

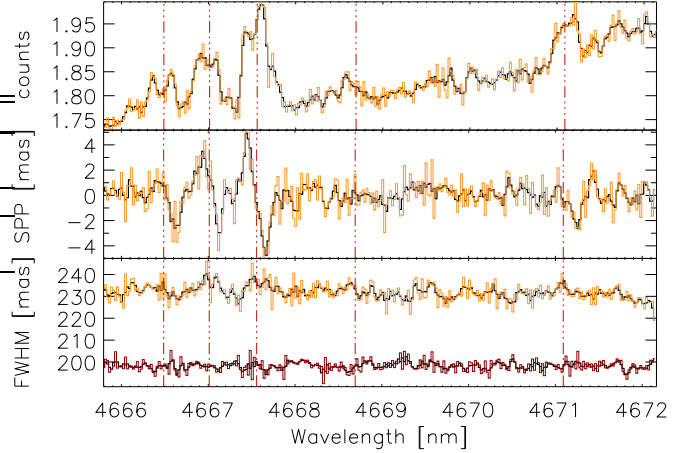


**Fig. 2.** *Top:* Close up of the spectrum of HD 97048 (as shown in Fig. 1). In all three windows the thick black line represents the original spectrum (orange thin line) smoothed over 2 pixels. Shown with the vertical dotted lines are the locations of the (from left to right)  $^{12}\text{CO}$  v(4-3) R23, v(3-2) R14, v(2-1) R06, v(5-4) R33 and  $^{13}\text{CO}$  v(1-0) R12 emission lines. *middle* The SPP. *Bottom:* The (spatial) FWHM of the PSF for each spectral row, as well as that of the telluric target in red.

ters listed in Table 1. We also over plot scaled high resolution ( $R = 80\,000$ ) data of [OI] 6300  $\text{\AA}$  emission from both disks, published by Acke & van den Ancker (2006). The average line profile and astrometric signal, model fit and [OI] emission for both targets are shown in Figures 4 and 5. The best fit parameters for the emission from the disks are inner and outer radii of 12 and 45 AU for HD 97048, and 17 and 40 AU for HD 100546. The average profiles of all vibrational bands have a FWHM of  $16\text{ km s}^{-1}$ , hinting that they originate from the same area. The [OI] emission has much wider wings, and originates from inner radii much closer to the star than the CO emission (80 % of the [OI] emission emanates from the region between 0.8 and 20 AU, Fig. 7 in Acke & van den Ancker (2006)).

We note that the shape of the averaged v(1-0) and v(2-1) profiles of HD 100546 differs from the higher vibrational transitions. The average line profiles appear as a single peak, whereas the individual higher vibrational transitions appear distinctly flattened or double peaked. This could be caused by emission originating from two regions. One region closer to the star, with higher projected velocity and temperature, and one further out with lower velocity and temperature. The superposition of these components, where the cold component fills in the central (low velocity) part of the line, can explain the observed profiles. To investigate this we also constructed average line profiles for both lines from the higher ro-vibrational transitions, shown with black dots in panels 1 and 2 of Fig. 5.

## 5. Discussion

Both stars show comparable CO line strengths, and modeling the CO emission in both cases suggests an emitting region between 12 and 45 AU. The sizes derived from the spatial FWHM, the SPP and the kinematic modeling for HD 97048 are consistent and show that the continuum emission comes from an area similar in size to that of the CO emission. The results from the kinematic modeling of HD 100546 show contributions from hot and cold gas for the lower vibrational lines. Its line

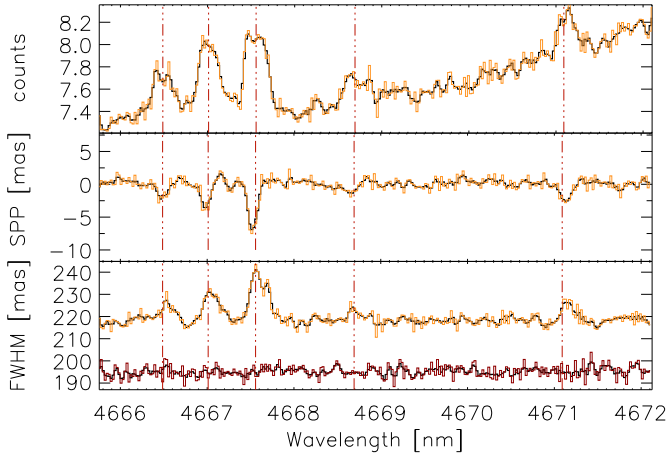


**Fig. 3.** Same as figure 2 for HD 100546

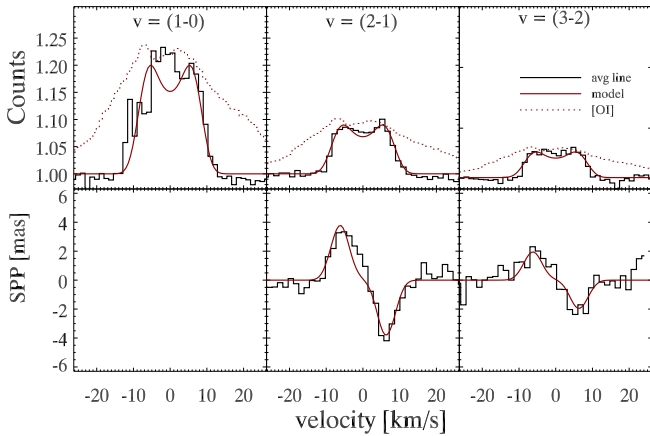


**Fig. 4.** *Top panels* The average line profiles of the HD 97048  $v(1-0)$ ,  $v(2-1)$  and  $v(3-2)$  transitions, created with resp. 5, 15 and 7 lines are shown with the black histogram. The deviating shape of the blue wing of the  $v(1-0)$  transition is caused by removal of overlapping telluric CO lines. Over plotted is the 6300  $\text{\AA}$  [OI] emission with red dots, and the model fit to the CO emission with the solid red line. *Bottom panel* The corresponding average astrometric signal for each transition, created with resp 12 and 7 lines. The astrometric model is over plotted in red. Due to overlapping telluric lines, it is not possible to construct the astrometric signal of the  $v(1-0)$  transition.

profiles, astrometric signals and spatial FWHM are asymmetric. This asymmetry has already been noted in the [OI] 6300  $\text{\AA}$  line by Acke & van den Ancker (2006), and may be due to a local enhancement in the CO emission, located in the part of the disk which is blue shifted. This increased gas density could be caused by a spiral arm (such as was observed by Ardila et al. (2007) in scattered light) or by a 'secondary wall' located at  $\approx 10$  AU from the star (Bouwman et al., 2003). The continuum emission of HD 100546 comes from a region twice as compact as that of HD 97048, whilst the CO emission originates from comparable radii.

Both our targets also display a lack of CO emission  $\leq 12$  AU. An inner hole has been detected in more circumstellar disks, e.g. in SR 21 with an inner radius of  $7.6 \pm 0.4$  AU for the  $^{12}\text{C}^{18}\text{O}$

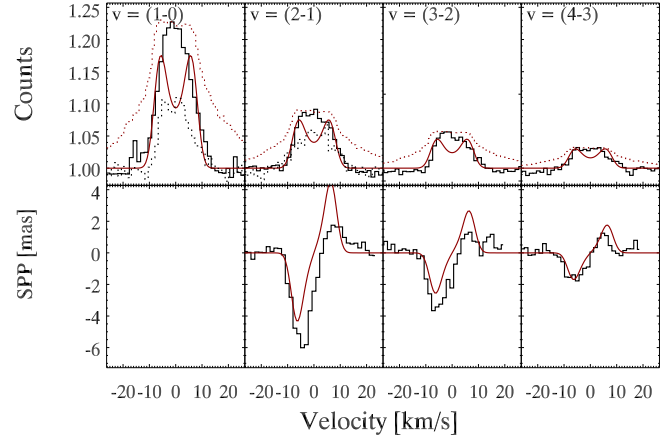


**Fig. 5.** *Top panel* Same as Fig. 4 for HD 100546, but the  $v(1-0)$ ,  $v(2-1)$ ,  $v(3-2)$  and  $v(4-3)$  profiles are made from resp. 9, 14, 10 and 8 lines. Over plotted in the  $v(1-0)$  and  $v(2-1)$  panels is the average line profile created from 5 high J ( $27 < J < 36$ ) ro-vibrational transitions. *Bottom panel* Same as Fig. 4 for HD 100546, but the  $v(2-1)$ ,  $v(3-2)$  and  $v(4-3)$  profiles are made from resp. 12, 8, and 13 lines.

$v(1-0)$  line (Pontoppidan et al., 2008), whereas there is a dust ring between 0.25 and 0.45 AU, followed by a dust gap up to 18 AU (Brown et al., 2007), and HD 141569, where Brittain et al. (2007) infer a minimal amount of both gas and dust within 6 AU. Unlike that disk however, the lack of CO emission in HD 97048 and HD 100546 can not be caused by a cleared inner disk. The [OI] 6300  $\text{\AA}$  emission, a tracer of molecular gas in the surface layers of flared disks and induced by the stellar UV field, has been observed for both stars by Acke & van den Ancker (2006), and modeling suggests that 80% of the emission originates between  $0.8 < R < 20$  AU. The SEDs of our targets also display large NIR excesses, typical for hot dust close to the star (Acke & van den Ancker, 2004; Bouwman et al., 2003). In the cases of HD 97048 and HD 100546, the absence of CO emission can therefore not be attributed to the paucity of matter in the inner disk, nor to the absence of UV flux. We suggest two possible explanations. While gas and dust are clearly present at small radii in both disks studied here, CO gas may be efficiently destroyed at radii smaller than 12 AU. A possible explanation is the higher temperature and density closer to the star, which may drive a rich chemistry in the disk, so that CO may be replaced by other species (e.g.  $\text{CH}_4$ ) as the dominant reservoir of carbon. Alternatively, radiative transfer effects could suppress the line emission from the innermost region. Further analysis (e.g. observations of hot transitions of carbon-bearing molecules) is needed to determine the reason why the CO gas is not detected in the inner regions, and may offer us a first glimpse of the molecular chemistry of the inner disk.

**Acknowledgements.** The authors of this paper wish to thank the Paranal night-time astronomer E. Valenti for her cheerful assistance making the observations.

## References

- Acke, B., & van den Ancker, M. E. 2004, *A&A*, 426, 151  
 Acke, B., & van den Ancker, M. E. 2006, *A&A*, 449, 267  
 Acke, B., van den Ancker, M. E., Dullemond, C. P., van Boekel, R., & Waters, L. B. F. M. 2004, *A&A*, 422, 621  
 Ardila, D. R., Golimowski, D. A., Krist, J. E., Clampin, M., Ford, H. C., & Illingworth, G. D. 2007, *ApJ*, 665, 512

- Boogert, A. C. A., Hogerheijde, M. R., & Blake, G. A. 2002, *ApJ*, 568, 761
- Bouwman, J., de Koter, A., Dominik, C., & Waters, L. B. F. M. 2003, *A&A*, 401, 577
- Brittain, S. D., Simon, T., Najita, J. R., & Rettig, T. W. 2007, *ApJ*, 659, 685
- Brown, J. M., et al. 2007, *ApJ*, 664, L107
- Carmona, A., van den Ancker, M. E., Henning, T., Goto, M., Fedele, D., & Stecklum, B. 2007, *A&A*, 476, 853
- Brannigan, E., Takami, M., Chrysostomou, A., & Bailey, J. 2006, *MNRAS*, 367, 315
- Dullemond, C. P., & Dominik, C. 2004, *A&A*, 417, 159
- Geers, V. C., van Dishoeck, E. F., Visser, R., Pontoppidan, K. M., Augereau, J.-C., Habart, E., & Lagrange, A. M. 2007, *A&A*, 476, 279
- Goto, M., Usuda, T., Dullemond, C. P., Henning, T., Linz, H., Stecklum, B., & Suto, H. 2006, *ApJ*, 652, 758
- Habart, E., Testi, L., Natta, A., & Carillet, M. 2004, *ApJ*, 614, L129
- Käufel, H.-U., et al. 2004, *Proc. SPIE*, 5492, 1218
- Kurucz, R. L. 1991, *Precision Photometry: Astrophysics of the Galaxy*, 27
- Lagage, P.-O., et al. 2006, *Science*, 314, 621
- Martin-Zaïdi, C., Lagage, P.-O., Pantin, E., & Habart, E. 2007, *ApJ*, 666, L117
- Meeus, G., Waters, L. B. F. M., Bouwman, J., van den Ancker, M. E., Waelkens, C., & Malfait, K. 2001, *A&A*, 365, 476
- Mitchell, G. F., Maillard, J.-P., Allen, M., Beer, R., & Belcourt, K. 1990, *ApJ*, 363, 554
- Najita, J., Carr, J. S., & Mathieu, R. D. 2003, *ApJ*, 589, 931
- Pontoppidan, K. M., Blake, G. A., van Dishoeck, E. F., Smette, A., Ireland, M. J., & Brown, J. 2008, *ApJ*, 684, 1323
- Salyk, C., Blake, G. A., Boogert, A. C. A., & Brown, J. M. 2007, *ApJ*, 655, L105
- van Boekel, R., Waters, L. B. F. M., Dominik, C., Dullemond, C. P., Tielens, A. G. G. M., & de Koter, A. 2004, *A&A*, 418, 177
- van den Ancker, M. E., de Winter, D., & Tjin A Djie, H. R. E. 1998, *A&A*, 330, 145